Recovery of Manganese Ions from Aqueous Solutions with Cyanex 272 Using Emulsion Liquid Membrane Technique: A Design of Experiment Study

Iman Salahshoori[1] · Ahmad Seyfaee[2] · Aziz Babapoor[3] · Ilaria Cacciotti[4]

Abstract

Manganese (Mn) is one of the most widely used metals in industry, even if it is highly toxic. Thus, the accumulation of manganese-containing wastes is one of the main environmental concerns. For this reason, its recovery from aqueous solutions is of particular importance and is gaining a lot of interest. Among the water treatments, emulsion liquid membrane (ELM) presents several advantages, such as ease of use, high efficiency, and single-step extraction. Therefore, the ELM technique has a high potential to replace the conventional methods for removing heavy metal ions, particularly for its high removal efficiency. The present research aims to analyze the feasibility of manganese ions removal from the water via the ELM method. Therefore, in the first step, the physicochemical factors affecting the stability of the liquid membrane were investigated. Then, the fractional factorial design (FFD) method was used to screen and choose the pivotal, influential factors on manganese ion extraction, such as carrier concentration, emulsion-to-feed phase volume ratio, feed phase pH, water-in-oil-in-water (W/O/W) emulsion stirring time and speed. Based on the collected results, the maximum extraction ($>97\%$) was achieved when the carrier concentration, emulsion/feed phase volume ratio, feed phase pH, W/O/W emulsion stirring time, and W/O/W emulsion stirring speed were $\sim 8\%$ v/v, ~ 3, ~ 4, ~ 17 min, and ~ 450 rpm, respectively.

Graphical Abstract
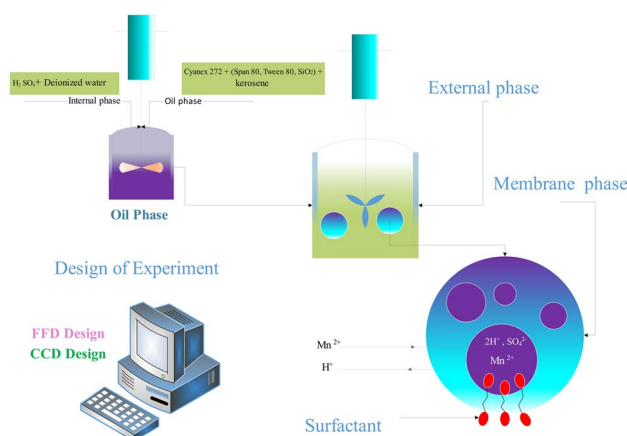
Keywords Manganese · Extraction · Emulsion liquid membrane · Cyanex 272 · Design of experiment

The contributing editor for this article was Hongmin Zhu.

Extended author information available on the last page of the article

Introduction

The emergence of industries and the irregular increase in urban population, followed by the development of agricultural areas, have increased urban, agricultural and industrial wastewater production containing various chemical compounds that could enter the aquatic ecosystem. Among these pollutants, heavy metals are of particular importance due to their high toxicity and adverse environmental impacts [1]. Therefore, removing heavy metal ions from wastewater has become an increasingly important issue in the past few decades due to economic and ecological considerations [2].

Among the heavy metals, manganese (Mn) is strategic due to its applications in various industries such as alloy makings, renewables (e.g., solar panels) and catalysts production. Therefore, it is highly likely to find some amounts of Mn ions in the industries' waste streams, with consequent dramatic environmental impact and concerns. For this reason, its recovery from aqueous solutions is of particular importance [3].

The most common methods in pollutants removal are precipitation [4], adsorption [5], reactive distillation [6], electrodialysis [7], liquid–liquid extraction (solvent extraction) [8], and ion exchange [9]. The mentioned conventional separation techniques are not advantageous due to sewage, solid waste production, sludge treatment and disposal, high consumption rate of chemicals, high capital and operating cost, and chemical agent recycling complexity [10].

Nowadays, it is common to use membrane-based separation processes to overcome some of the declared disadvantages. The membrane separation processes are beneficial due to their low maintenance cost, ease of use and cleaning, and low energy consumption [11–15]. Liquid membrane-based separation technology has increasingly become a viable option for various separation processes due to its benign environmental impacts [16]. Among different liquid membrane techniques, emulsion liquid membrane (ELM) is considered a promising separation method due to its low cost, low energy consumption, large specific surface area, and high mass-transfer rate [17].

Particularly, it should be noted that the separation via ELM could be desirable as it simultaneously extracts, removes, and transfers the contaminants in one step from a large volume to a relatively small volume [18]. Moreover, emulsion liquid membranes can be used for the removal/extraction of various salts, metal ions, organic acids, amines from waste streams, and separation of hydrocarbons [19–22]

The ELM process consists of three essential phases [19–21]:

- internal phase (stripping phase): a dispersed aqueous phase that is made up of stripping agents, deionized water, and the carried heavy metal ions;
- external phase: a continuous phase of the feed, which is the source of contaminant metal ions;
- membrane phase: a dispersed organic phase that separates the internal phase droplets from the external phase's emulsion and usually consists of three components(i.e., diluent, surfactant (stabilizers), and carriers (that carry metal ions from the external phase to the internal phase)).

It should be noted that despite the effectiveness of this method in the laboratory, its commercial application in the removal of heavy metals has been limited and precluded due to the emulsion membrane instability [23] associated with membrane leakage and emulsion swelling. The main consequence of emulsion instability is the reduction in the extraction process's efficiency [24].

Thus, in the appropriate choice of membrane formulation (organic phase), the mixing with suitable additives and surfactants and increasing the membrane phase's viscosity are pivotal aspects to potentially reduce the instability of emulsion liquid membrane [25]. Simultaneously, it is essential to select the appropriate materials in the ELM process to achieve the highest recovery percentage.

Concerning the carrier, Cyanex families are widely used in the separation process of metals in hydrometallurgy. Cyanex 272 is considered in this work due to stability against heat and hydrolysis, high solubility in aromatic and aliphatic solvents.

For the organic phase membrane, diluents are one of the main components. Although diluents must have low solubility in water, they should provide high solubility for the carrier, have a high boiling point, suitable density, viscosity, flash point, polarity, low toxicity, and low cost [16, 17]. Among the most widely used diluents, kerosene [26] has been used as an organic diluent due to its favorable viscosity, ease of availability, and non-polar properties. Surfactants, as another component of ELMs, should provide stability in the emulsion structure. In addition to the proper selection of surfactants, the use of surfactants/nanoparticles mixture in the liquid membrane phase could increase membrane stability [27]. Davoodi-Nasab et al. [28] used a combination of Span 85 and multi-walled carbon nanotubes (MWCNTs) to improve emulsion stability in gadolinium ion extraction, using Cyanex 272 carrier. In another study, Raji et al. [29] used MWCNTs and Span 80 mixtures to increase the stability of liquid membranes devoted to the dysprosium removal.

The choice of the internal phase (stripping phase) is another key factor in the separation via the ELM method. The internal (stripping) phase has two important characteristics: (i) compatibility with other components used in ELM to

increase the membrane stability and (ii) formation of a very stable complex with metal ions.

In this framework, the present work aims to investigate the feasibility of manganese ions removal from water via the ELM method. To achieve this aim, in the first step, the physicochemical factors affecting the stability of the emulsion liquid membrane were investigated, using one factor at a time (OFAT). Then, a design of experiment (DOE) analysis was performed through a fractional factorial design (FFD) approach, which was used as the screening method to identify the most influential factors on the experimental results (e.g., carrier concentration, emulsion-to-feed phase volume ratio, feed phase pH, water-in-oil-in-water (W/O/W) emulsion stirring time, and speed) [30]. Finally, response surface methods (RSMs) were employed to examine the levels of influencing factors. Central composite design (CCD), as one of the most widely used RSMs due to its versatility, was applied to compare the OFAT and CCD method results [31].

The OFAT method shows several drawbacks: it is mainly based on trials and errors, it usually does not follow any specific methodology, and, mainly requires a large number of tests. Thus, DOE is suggested as an addition or replacement to OFAT to overcome the mentioned shortcomings in the OFAT method, which, for example, could lead to evaluation of the membrane's performance and identify the optimal conditions with fewer tests [32].

So far, to the best of our knowledge, no research has been performed to investigate the emulsion stability and recovery of manganese ions using ELM via the DOE method up to date.

Materials and Methods

Materials

Manganese II sulfate anhydrous (GR grade Merck) was used to prepare the feed (external) phase. Sulfuric acid (H_2SO_4), perchloric acid ($HClO_4$), nitric acid (HNO_3), and hydrochloric acid (HCl) (all from Merk) were used as the internal phase. Sorbian monooleate (Span 80), polysorbate 80 (Tween 80) and silica (SiO_2) (all supplied from Sigma-Aldrich Co.) were used as emulsion stabilizers. Bis (2,4,4) trimethylpentyl phosphinic acid (Cyanex 272, Cytec Co., Canada) was applied as the carrier. Kerosene, n-heptane, and 1,2-dichloroethane (Sigma-Aldrich Co.) were utilized as an organic phase. Nitric acid (HNO_3) and sodium hydroxide (NaOH) were used for adjusting pH (Merck Co.). Deionized (DI) water was used in all solutions preparation and in the performed tests.

Apparatus

Shin Saeng laboratory stirrer (model SDS-41D, Korea) was used to mix the solutions during the extraction process. A shaking water bath (model SWBR27, Shel lab Co.) was used to monitor the temperature. A laboratory homogenizer (T25 digital ultra-Turrax, model IKA) was employed to prepare the initial emulsion. A Malvern Zeta sizer was used to measure nanoemulsion's size distribution by means of the dynamic light scattering (DLS) method. A 3505 pH meter (Jenway Co.) was used to measure the pH of aqueous solutions. The concentration of manganese ions in feed samples was measured using an atomic absorption spectroscopy (AAS) AA300 (Perkin Elmer Co.). Infrared spectroscopy (Bruker Tensor 27, USA) (FTIR) was used in the wavenumbers range of 400 to 4000 cm^{-1} to investigate the functional groups present in the membranes.

Procedure

Figure 1 represents the schematic view of the ELM process for manganese separation. In the first step, the internal and membrane phases should be mixed to construct the W/O emulsion. Hence, various acid solutions, such as $HClO_4$, HNO_3, HCl, and H_2SO_4, with concentrations ranging from 0.2 to 2 M, were prepared as the internal phase. Then surfactants (SPAN 80, TWEEN 80), carrier material (Cyanex 272), and SiO_2 nanoparticles with different concentrations were added to the diluent (kerosene) to form the organic (membrane) phase. The internal phase was added dropwise to the organic (membrane) phase under severe agitation at different rates (ranging from 8000 to 14,000 rpm) using the lab homogenizer to make the W/O emulsion. Moreover, a solution of 500 ppm manganese sulfate was prepared as the external (feed) phase.

Nitric acid (0.1 M) and sodium hydroxide (0.1 M) were used to adjust the external phase (feed phase) pH. Next, the primary emulsion (W/O) was added to the external phase containing the manganese ions. The extracting vessel was placed in a water bath to keep the temperature constant. Then sampling was performed at specific time intervals using 5 ml syringes. Afterwards, the samples were centrifuged to separate the organic phase from the feed phase. Measurement of the residual manganese content in the aqueous phase for each sample was done by atomic absorption spectroscopy at a wavelength of 172 nm. The extraction percentage (E%) of manganese ions concentrations was calculated using Eq. (1):

$$E\% = \left[\frac{C_0 - C_t}{C_0} \right] \times 100, \tag{1}$$

where C_0 is the initial metal ion concentration in the feed solution, and C_t is the metal ion concentration in the feed solution at time t

The stability of the emulsion was calculated via Eq. 2:

$$\text{Leakage} = \frac{V_R}{V_i^0} \times 100, \tag{2}$$

where V_i^0 is the initial volume of the internal phase and V_R is the volume of the leaked internal phase to the external phase and calculated via the following relation:

$$V_R = V_e^0 \times \frac{10^{pH_e^0} - 10^{pH_e^t}}{10^{pH_e^t} - C_{H+,i}^0}, \tag{3}$$

where V_e^0 is the initial volume of the external phase, $C_{H+,i}^0$ the initial concentration of H^+ in the internal phase, pH_e^0 the initial pH of the external phase, and pH_e^t the external phase pH collected via the separating funnel at any sampling time (t).

In the DOE analysis, the FFD method was firstly used to identify the factors affecting the manganese ion extraction process. FFD method at 1/2 level with a resolution of IV was used to reduce the number of experiments. For this purpose, the lower and upper levels of each factor were determined (Table S1). The software was designed with 32 test steps.

According to Table S2, the proposed points of each factor were identified. Then, the amount of manganese ion extraction in each step was obtained using Eq. 1. The analyses were then performed to identify the number of factors affecting the manganese ion extraction process. The design of the experiment using the CCD method was also carried out according to the instructions of the FFD method. In this way, the high and low levels of factors were introduced to the software (Table 1). Then, based on the experimental design matrix (Table S4), manganese ion extraction experiments were performed, and the desired analyses were carried out on the responses.

Results and Discussion

Membrane Stability

The stability of the ELM is one of the most important parameters and strongly affects the extraction performance. Membrane break-up causes a decrease in the separation efficiency due to the leakage of the separated ions from the internal to the external phase [33]. The main causes of emulsion breakage are osmotic swelling, coalescence, creaming, sedimentation, and flocculation of droplets. There are
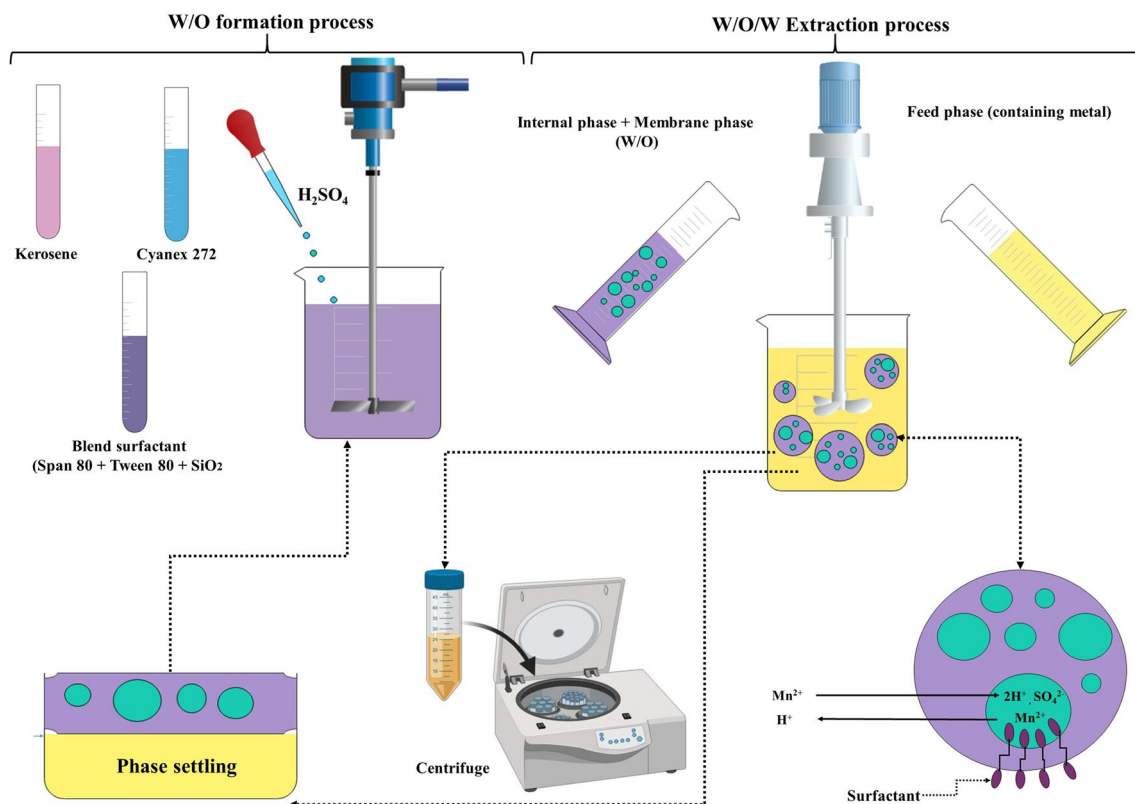

Fig. 1 A schematic of the experimental setup

several methods to increase emulsion stability. One way to improve emulsion stability could be using a mixture containing blended surfactants and nanoparticles [27]. Factors, such as emulsification rate and time, type, and concentration of the surfactant and the internal phase, and the internal phase/membrane phase volume ratio, affect the membrane stability. In this section, all the influencing factors on membrane stability and its separation performance are studied.

Effect of Diluent Type on ELM Stability

In this study, a few commercial diluents, widely used in the ELM system, were employed to investigate their effect on the emulsion stability in terms of leakage percentage *vs* contact time (min) (Fig. 2a–d). The commercial diluents used in this study were kerosene ($\mu = 1.3$ cP and $\rho = 810$ kg/m^3), n-heptane ($\mu = 0.386$ cP and $\rho = 684$ kg/m^3), and 1,2-dichloroethane ($\mu = 0.84$ cP and $\rho = 1253$ kg/m^3) [18]. Figure 2a shows the effect of the diluent type on the emulsion stability. As depicted in Fig. 2a, kerosene and n-heptane employment led to the most and the least emulsion stability, respectively. The greater stability of the emulsions evidenced in the case of kerosene could be due to its density (e.g., similar to water density) and viscosity (relatively high viscosity).

Effect of Emulsification Rate on ELM Stability

The rate of emulsion homogenization plays a pivotal role in emulsion stability and extraction efficiency. Figure 2b illustrates the effect of the emulsification rates on the stability of the W/O emulsion, investigating a homogenizer speed range of 8000–14,000 rpm. As presented in Fig. 2b, on the one hand, an increase in the homogenizer rate from 8000 to 12,000 rpm led to an increment in the efficiency of the membrane stability, which can be related to appropriate mixing and reduction of surface tension between the aqueous and organic phases, as well as an increase in the number of the droplets. On the other hand, with increasing the emulsification rate beyond 12,000 rpm, the membrane stability decreased, and a highly viscous, "creamy-like" emulsion was formed. This could be due to the foaming with the formation of several air bubbles in the emulsion due to severe agitation and, hence, a drastic increase of the emulsion viscosity.

Figure 3 demonstrates the DLS size distribution of W/O emulsion droplets at different emulsification rates (8000–14,000 rpm). It is observed that the mean intensity of the average droplet size monotonically decreased with increasing the emulsification rate from 27.5% (8000 rpm), 22.5% (10,000 rpm), 15% (12,000 rpm), and 12.5% (14,000 rpm). It is evident from Fig. 3 that with an increase in the emulsification rate, the droplet size decreases from ~96 nm (8000 rpm) to ~75 nm (10,000 rpm), ~42 nm (12,000 rpm), and ~18 nm (14,000 rpm).

Emulsification rate can have different effects on emulsion stability. In general, W/O emulsions with small diameter droplets tend to resist the phase separation and display relatively high stability. However, it should be noted that if the diameter of the W/O emulsion droplets is very small, in the extraction process (W/O/W), due to the presence of a more significant number of internal phase globules in the membrane phase, the liquid membrane becomes thinner and is followed by emulsion breakdown. In contrast, in W/O/W emulsion containing large diameter droplets, the separation efficiency decreases due to the droplets' coalescence, a low surface-to-volume ratio, and a low mass-transfer rate [34, 35].

## Effect of Emulsification Time on ELM Stability

Experiments were performed with different emulsification times in the range of 2.5–17.5 min to investigate its influence on ELM stability. Figure 2c demonstrates the effect of the emulsification time during the W/O emulsion preparation on its final stability. As depicted in Fig. 2c, the highest emulsion stability was obtained when the emulsification time for the preparation of W/O was 7.5 or 12.5 min. For an emulsification time less than 7.5 min, the membrane leakage rate was high, possibly due to the lack of homogenization of the internal phase droplets and their large diameter in the membrane [36]. However, a further increase in the emulsification time above 12.5 min led to a decrease in the membrane stability thanks to the formation of new emulsion interfaces and to the reduction in the available surfactant molecules unit area of the droplets [25]. Therefore, emulsification time of 12.5 minutes was considered to achieve sustainable emulsion stability.

Table 1 Levels of factors in the central composite design

Factor	Symbol	Unit	$-\alpha$	-1	0	$+1$	$+\alpha$
Emulsion/feed phase volume ratio	X_1		1	3	5	7	10
Carrier concentration	X_2	wt%	2	4	6	8	10
Feed phase pH	X_3		1	3	4	5	7
W/O/W emulsion stirring time	X_4	min	5	10	15	20	25
W/O/W emulsion stirring speed	X_5	rpm	250	350	450	550	650
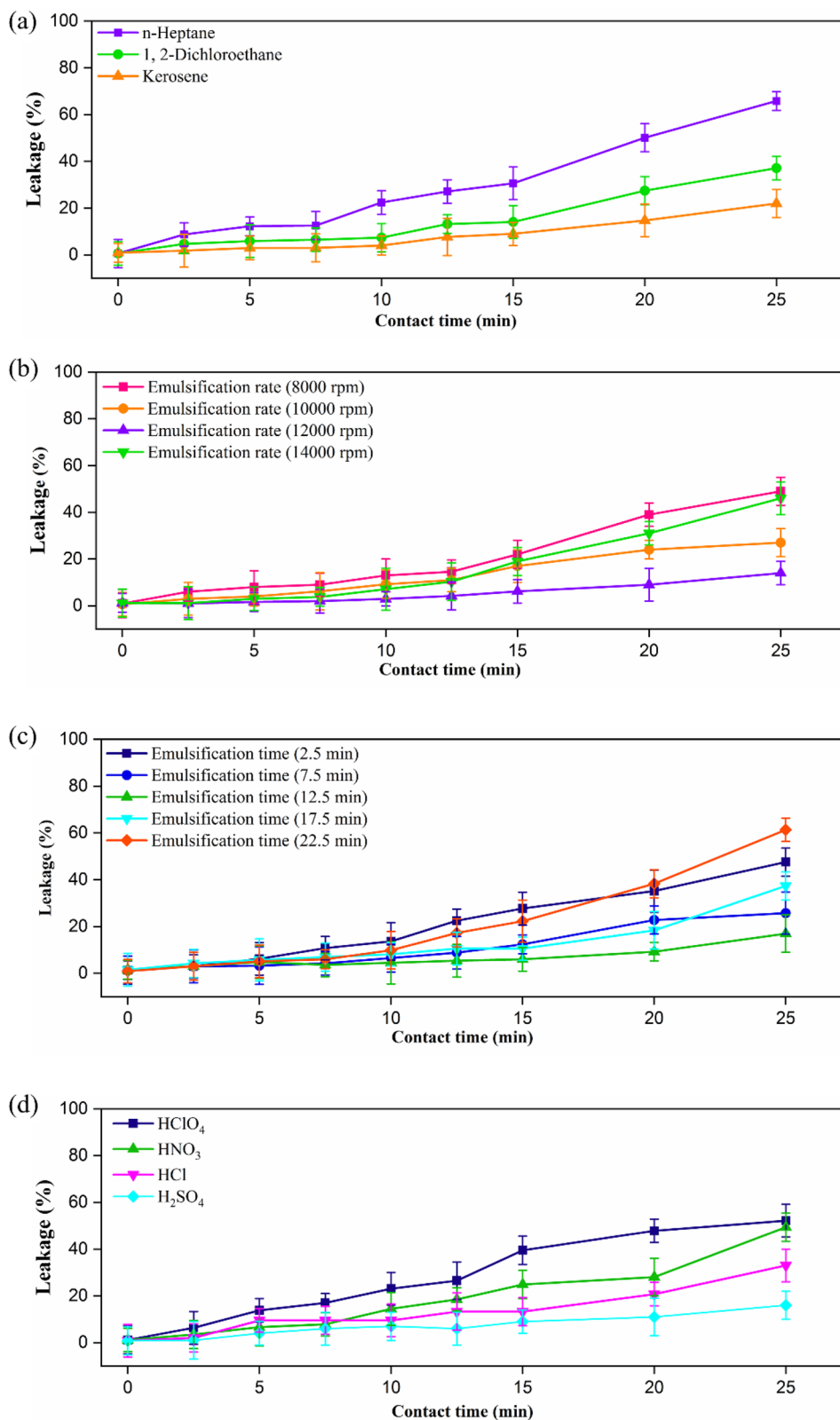
Effect of The Internal Phase Type on ELM Stability

Another practical influencing factor in ELM stability is the type of internal phase. In this regard, the effect of $HClO_4$, NH_3, HCl, and H_2SO_4 as internal phase on the membrane's stability was investigated. As shown in Fig. 2d, the membrane containing sulfuric acid as the internal phase was more stable than other membranes containing $HClO_4$, NH_3, and HCl. This increase in emulsion stability due to sulfuric acid can be attributed to the metal sulfates' higher solubility [36]. Hence, as evident in Fig. 2d, the emulsion stability decreased when metallic salts were formed in the receiving phases, disrupting the internal phase surface properties with a consequent higher chance of internal phase globules coalescence and, finally, membrane breakdown. Therefore, once the salts' formation in the receiving phase occurs, the membrane structure becomes unstable and breakdowns. Othman et al. [37] used sulfuric acid and hydrochloric acid in the internal phase and studied their impact on emulsion stability. They stated that the use of sulfuric acid in the internal phase increased the emulsion's stability compared to hydrochloric acid, in agreement with our results.

Effect of the Internal Phase Concentration on ELM Stability

Obtaining the internal phase's optimal concentration is of particular importance in studies on the emulsion stability in the ELM technique [38], and much research has been performed on this topic. Thus, in the present study, sulfuric acid solutions concentrations ranging from 0.1 to 2 M were tested. As depicted in Fig. 4a, the most stable W/O/W emulsion was obtained using 1 M sulfuric acid solution as the internal phase, and thus, 1 M was selected as the optimal internal phase concentration. Indeed, with an increase in the internal phase concentration from 1 to 2 M, the emulsion stability decreased. It should be noted that the decrement of

the emulsion stability with increasing the internal phase concentration may be related to the osmotic swelling [25, 39].

Comparable results were reported in previous research works. Fouad et al. evidenced that the most stable emulsion in the zinc ion extraction tests was achieved when a 1.5 M sulfuric acid solution was used as the internal phase [40]. Gasser et al. [41] obtained the optimal EML stability in cobalt ion extraction with a sulfuric acid solution concentration of 0.5 M.

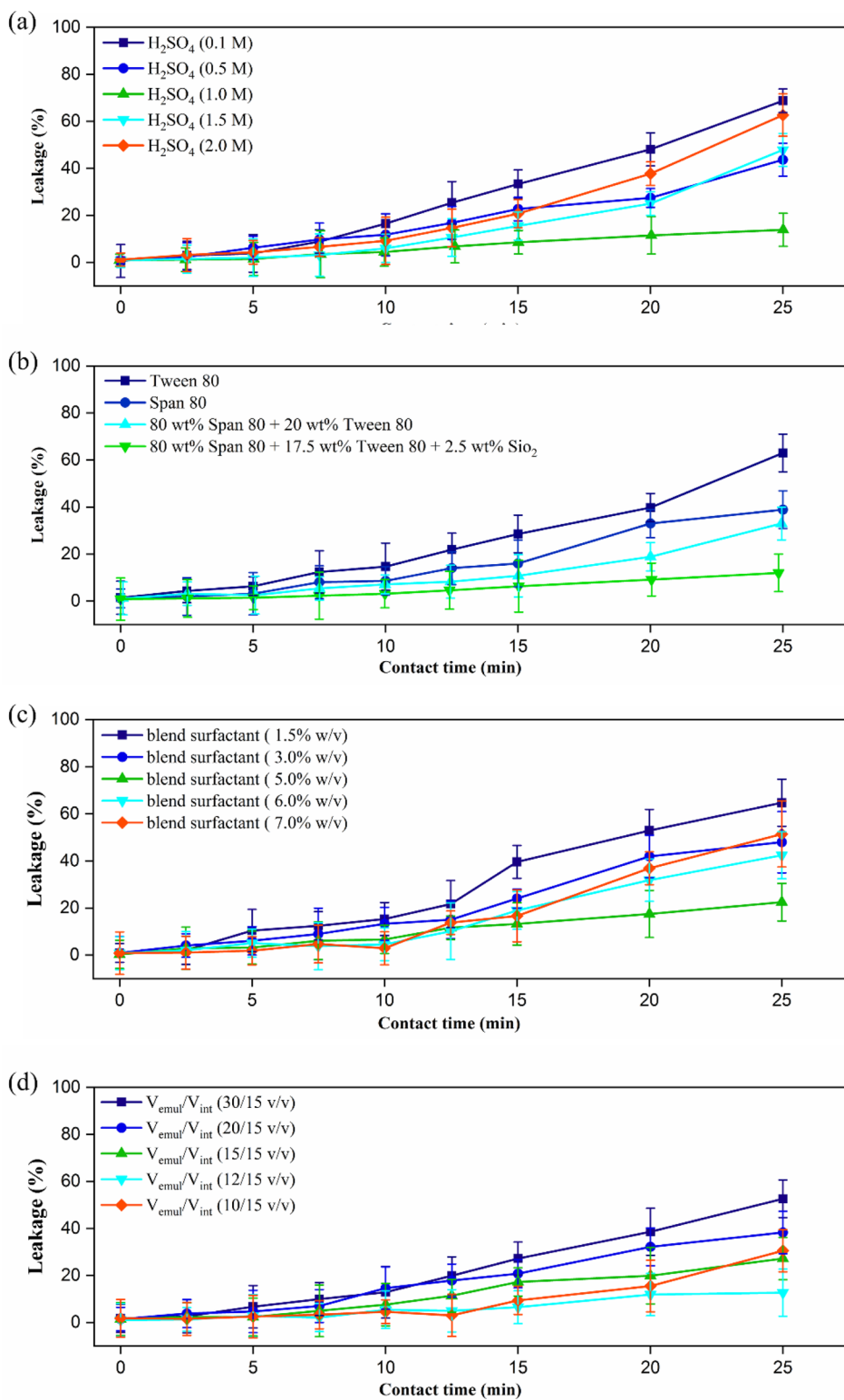## Effect of the Surfactant Type on ELM Stability

The selection of suitable surfactants types and their optimal concentrations could improve the emulsion stability, reducing the swelling behavior and emulsion breakage, and, thus, facilitating the ion metal extraction [42]. Indeed, the addition of surfactants leads to a reduction in the surface tension between phases due to their liquid–liquid interface positioning [43, 44].

In this study, two types of surfactants, Span 80 and Tween 80, and a combination of them were used to evaluate the influence of the surfactant type on the stability degree. In addition, silica nanoparticles were used to enhance the emulsion stability and performance of the ELM system. As illustrated in Fig. 4b, the use of Tween 80 produced the least stable emulsion compared to Span 80, perhaps due to its lower solubility in the organic phase and lower hydrophobicity [45]. As shown in Fig. 4b, mixing 20 wt% of Tween 80 to 80 wt% of Span 80 enhanced the emulsion stability. This increase in stability can be attributed to the Tween 80 and Span 80 molecules' synergistic relationship, which leads to the creation of a stable network, reducing the droplets coagulation and ultimately preventing emulsion breakage [45, 46]. Moreover, the results showed that the addition of silica particles improved the stability of the membranes to the extent that, even after the extraction time of 20 min, the

Fig. 3 DLS size distribution of W/O emulsions at different emulsification rate in the range 8000–14,000 rpm
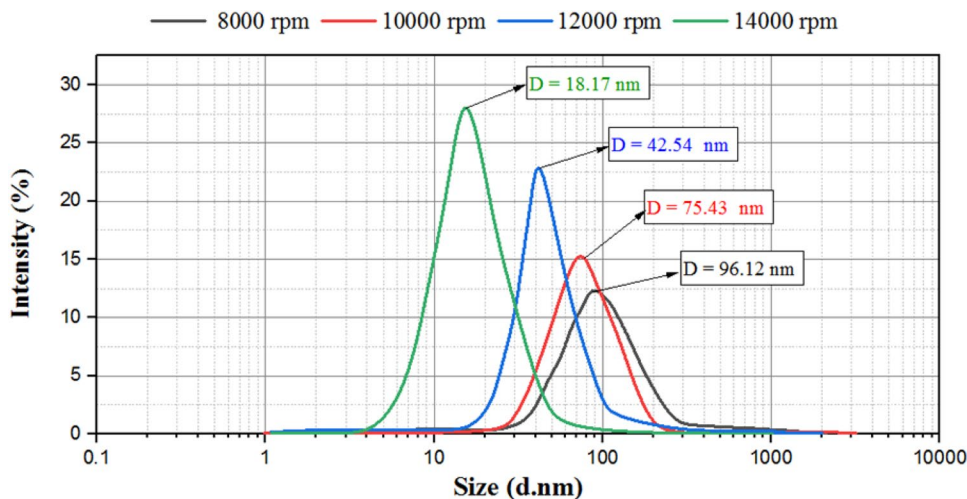
Fig. 4 Effect on the emulsion stability of **a** internal phase concentration, **b** surfactant type, **c** surfactant concentration, and **d** membrane phase volume ratio to internal phase. (All experimental conditions used of each factor in the ELM stability section were reported in Table S5)

leakage remained below 15%. It should be noted that the membrane leakage for different considered cases became evident when the extraction duration was more than 7 min.

Effect of the Surfactant Concentration on ELM Stability

Apart from the surfactant type, the surfactant concentration plays a significant influence on the emulsion stability. In this study, the effect of surfactant concentration in the range of 1 to 7% (w/v) on the emulsion stability was investigated. As shown in Fig. 4c, emulsion stability increased with increasing surfactant concentration from 1.5 to 5% (w/v). However, with a further increase in the surfactant concentration beyond 5%, the emulsion stability decreased. In general, with increasing the surfactant concentration, the surface tension between the phases decreases, which leads to an increase in the stability of the smaller droplets and the emulsion [47]. However, when the surfactant concentration passes a threshold, i.e., critical micelle concentration (5% w/v in this study), it promotes the formation of the reversed micelles in the aqueous phase, which in turn facilitates the aggregation of the globules and, therefore, destabilizes the emulsion [18]. Moreover, the internal phase's osmotic pressure could increase with the surfactant concentration and lead to the membrane phase's swelling and breakages. Therefore, 5% v/w was chosen as the optimum value.

Effect of Volume Membrane Phase to the Internal Phase Ratio on ELM Stability

The organic (membrane) phase to the internal phase volume ratio is another factor to monitor the emulsion stability. As depicted in Fig. 4d, the emulsion stability increases with an increase in phases' volume ratio. On the one hand, a low volume ratio could not encapsulate the internal phase droplets, thus, producing larger droplets diameters. Therefore, this resulted in the formation of a thinner membrane layer that adversely impacted the membrane stability. On the other hand, an increase in the volume ratio of organic phase to internal phase beyond 12:15 (v/v) formed a polydispersed emulsion with a large enough droplet diameter to promote instability and break into a film rather than dispersed globules. Therefore, to prepare a more stable W/O/W emulsion, which may contain a more uniform globule, the volume ratio of 12:15 (v/v) was considered.

Selection of the Essential Factors Influencing the ELM Process

Fractional factorial design (FFD) was used to screen and identify the experimental results' influential factors. The factors expected to affect the treatment via the ELM method, with their specified high and low levels, are collected in Table S1. Minitab 18 software was used to design the experiments through the FFD method. Manganese removal percentage was selected as the response. The design matrix following with the percentage of manganese removal in each test is presented in Table S2. Fig. S1a, b depicts the Pareto graph and typical plot which are used in the determination of factor significance in the FFD method. As demonstrated in Fig. S1a, factors such as W/O/W emulsion stirring time (J), W/O/W emulsion mixing rate (K), carrier concentration (D), and feed phase/emulsion volume ratio (G) were more effective than the other factors. Furthermore, as shown in the normal plot (Fig. S1b) and as reported in Table S3, it is evident that the pH of the feed phase (A) exerts a significant effect on both the organic/H_2SO_4 volume ratio factor (E) and emulsion volume/feed phase ratio factor (G). The resultants of these two factors (AE and AG) significantly affect the response rate. Therefore, feed phase pH (A) was also selected as one factor influencing the response rate.

Investigating the Influence of the Selected Major Factors on Manganese Extraction

Carrier Concentration

As shown in Fig. 5a, with an increase in the carrier material concentration from 0 to 7.5% (v/v), the Mn extraction rate increased. However, by increasing the carrier concentration from 7.5% (v/v) to 10% (v/v), the extraction rate decreased. Indeed, by excessively increasing the carrier concentration, the membrane phase's viscosity increases, resulting in elevating the resistance against mass transfer and reducing the extraction efficiency [36]. The carrier in the membrane phase plays two important tasks:

- the transmission of manganese ions between the external phase (feed) and the internal phase (stripper) within the membrane phase;
- the improvement of the ELM process selectivity.

On the one hand, if the carrier concentration is low, the extraction rate is low due to the lack of complex formation to transfer the heavy metal ions. Additionally, the presence of the carrier molecules in the membrane phase may decrease the emulsion stability as they compete with the surfactants to be adsorbed at the interface of the internal phase and the membrane phase [48]. On the other hand, if the carrier concentration increases to a certain extent, the viscosity increases. Due to a decrease in mass transfer, the extraction efficiency decreases [49]. The carrier concentration of 7.5% was chosen as the optimal concentration in this work.

Emulsion (W/O) Phase to Feed Phase Volume Ratio

The emulsion (W/O) phase/feed phase volume ratio plays a vital role in the extraction process and strongly influences the amount of extraction by emulsion. As illustrated in Fig. 5b, increasing the volume ratio of the W/O emulsion (made up of the internal phase and the membrane phase) to feed phase from 1/10 (v/v) to 2/10 (v/v) in the external phase slightly improved the extraction rate. However, increasing the emulsion to external phase volume ratio beyond 2/10 decreased the extraction rate. Generally, with an increase in the volume ratio of the W/O emulsion to feed phase, the membrane capacity for Mn separation, the mass-transfer rate, and the number of W/O/W globules would increase, and consequently enhance the separation rate. However, increasing the emulsion amount in the feed would introduce more internal phase droplets with their acidic content and hence facilitate the leakage of the internal phase, resulting in a reduced extraction rate of Mn ions [50, 51]. Therefore, the best ratio of the emulsion phase volume to the external phase was considered to be more than 2 to 10 (100 to 500 ml) to extract more manganese ions.

W/O/W Emulsion Stirring Rate

Another important factor affecting the membrane stability and extraction efficiency in the ELM process is the stirring rate of W/O/W emulsion. On the one hand, increasing the mixing rate can form smaller globules, improve the mixture's uniformity (i.e., reduce the swelling of internal phase droplets), and decrease the separation process's mass-transfer resistance. In fact, since the mass transfer within the membrane controls the ELM process's mass transfer, a reduction in the membrane droplets could increase the extraction efficiency [52, 53]. On the other hand, this increase in speed could lead to a rise in the emulsion cells' breakage due to increased mechanical interaction.

In general, it is important to stir the emulsion at the appropriate rate and keep it steady during the test to maintain the membrane stability and minimize emulsion swelling and breakage [54]. As shown in Fig. 5c, the stirring rate's extraction efficiency at 450 rpm was the highest for any given contact time.

W/O/W Emulsion Stirring Time

The rate of mass transfer and extraction is directly related to the contact time. On the one hand, a stirring time rise can increase the mass transfer and the rate of extraction. On the other hand, an excessive increase in the contact time leads to a reduction in the extraction rate due to the internal phase's leakage into the external phase. It should be noted that the extraction rate would be maximum in the early stages of the process due to the high rate of mass transfer [20, 55]. As time increases, droplets' swelling rises, increasing the internal phase volume and causing the emulsion to disintegrate. The high contact time increases the emulsion's water transfer rate and the emulsion [20, 55]. According to Fig. 5d, the extraction rate increased initially with increasing contact rate.

Nevertheless, after 15 min, the extraction rate gradually decreased. As time increased, the ELM became less stable (perhaps due to swelling), and the extraction rate decreased. Therefore, 15 min is the best time for the W/O/W emulsion stirring time factor to achieve the maximum amount of manganese ion extraction.

Feed Phase pH

It is stated that the H^+ concentration difference between the two aqueous phases (i.e., internal and external phases) plays an important role in the extraction of the metal ions [56, 57]. The amount of manganese dissolution in the organic phase directly depends on protons' concentration in the external phase [36]. In this research, a pH range between 1 and 7 was tested for the feed phase. The manganese ions began to precipitate in the form of manganese sulfate salt at pH above 8. Hence, the primary internal phase (e.g., NH_3) was not suitable for testing. Besides, very acidic environments caused emulsion breakdown and low manganese ion extraction. It should be noted that the mass transfer of metal ions occurred when the pH in the internal phase was lower than that of the external phase. As depicted in Fig. 5e, the best extraction conditions occurred at pH 4.

Investigation of Selected Minor Factors for the Manganese Extraction

In addition to the primary factors reported in Sect. 3.3, the effect of other identified parameters on the Mn separation was studied. 500 ppm was considered as manganese sulfate concentration in the external phase. According to the stability experiments, a mixture composed of 80 wt% Span 80, 15 wt% Tween 80, and 5 wt% silica provided the highest stability and was selected as the optimal surfactant stabilizer concentration in the extraction tests. The volume ratio of the organic (membrane) phase to the internal phase is equal to 12/15 (v/v) resulted in the optimum ratio. The optimal duration and rate for W/O emulsification were found to be ~ 12 min and 12,000 rpm, respectively, and considered for the experiments optimization.

Fig. 5 Effect on the extraction ratio of Mn (II) of **a** carrier concentration, **b** emulsion volume/feed phase ratio, **c** W/O/W emulsion stirring speed, **d** W/O/W emulsion stirring time, and **e** feed phase pH. (All experimental conditions used of each factor in the manganese extraction section was reported in Table S5)
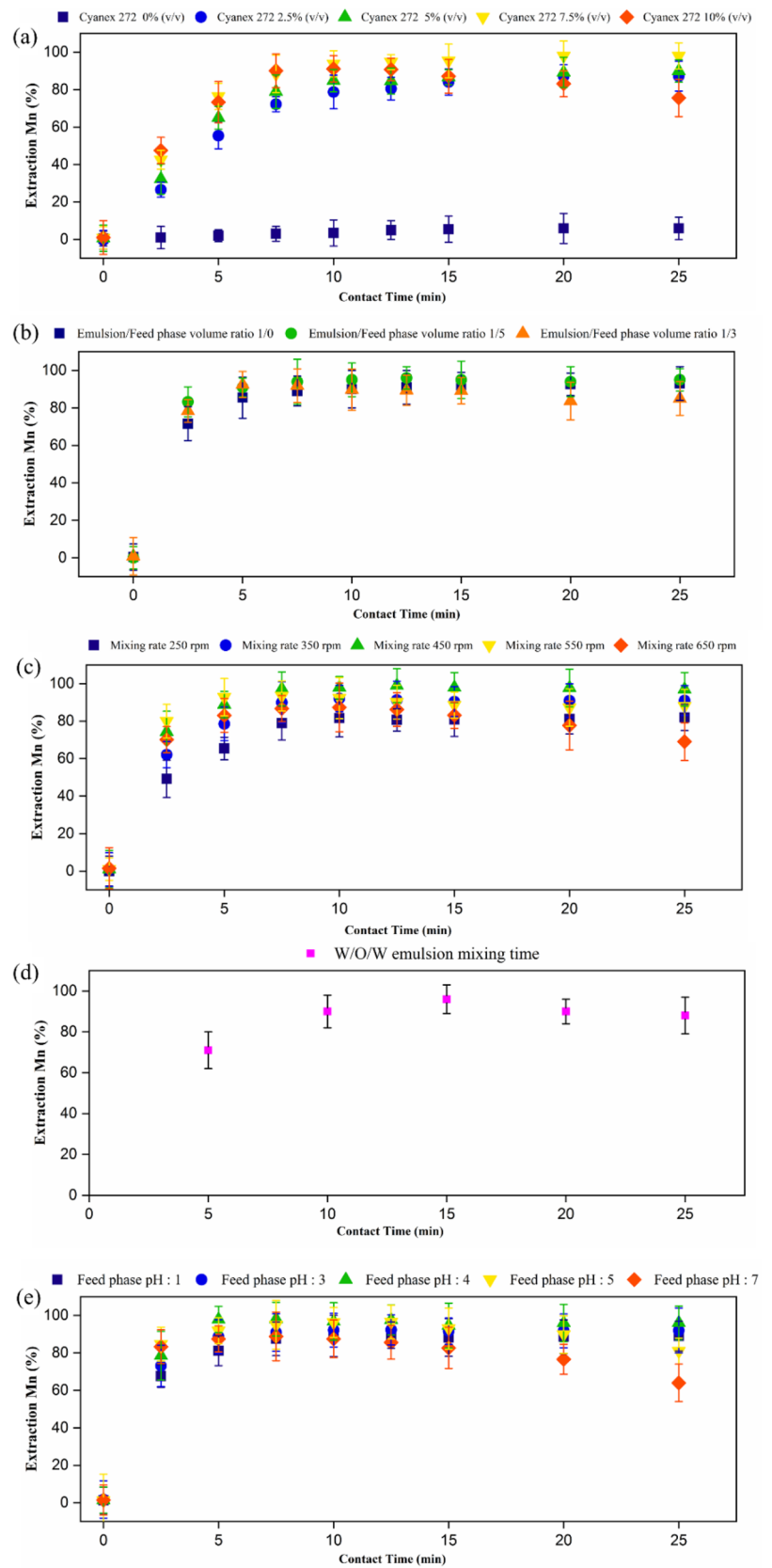
Mechanism of the Manganese Ions Separation

Extraction by Cation Exchange (Extraction by Acidic Carrier)

In a cation exchange extraction system, the extraction of a cation is accompanied by substituting a number of extraction molecules equivalent to that cation's electric charge. Groups of organic molecules that contain exchangeable protons are called acidic carriers (cation exchangers). For the extraction of M^{n+} metal ion by acidic extractor (HL), the reaction can be written as follows[58]:

$$M^{n+}_{aq} + nHL_{org} \leftrightarrow ML_{n,org} + nH^+_{aq},$$
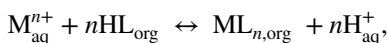
where $M^{(n+)}_{aq}$, HL_{org}, $ML_{(n,org)}$ and nH^+_{aq}, are the metal ions in the feed, the used carrier, the ion metal-carrier complex, and the hydrogen ions released during metal complex formation, respectively. For manganese metal, the constant n is equal to 2, that is, the Mn normal oxidation number. The equilibrium constant, K_{ex}, based on the reported reaction, would be

$$K_{ex} = \frac{[ML_n]_{org} [H^+]^n_{aq}}{[M^{n+}]_{aq} [HL]^n_{org}}. \tag{4}$$

In addition, the ratio of coefficient distribution (D) is defined as follows (Eq. 5):

$$D = \frac{[ML_n]_{org}}{[M^{n+}]_{aq}}. \tag{5}$$

By substituting the distribution coefficient in Eq. 4 in a logarithmic form, Eq. 6 will be obtained:

$$\log D = \log K_{ex} + n \log [HL]_{org} + n pH. \tag{6}$$

By plotting the log D vs log [Cyanex 272] (concentration of the used carrier), with the pH constant (pH 4), a linear slope equal to the number of acidic ligands in the extraction complex is obtained (Fig. 6a). The obtained plot perfectly matched a straight line with a slope of 2.01 ($R^2 = 0.99$), indicating that the ion exchange with 2 mol of the Mn (II) ions in the extraction process is possible and confirms the extraction equilibrium reaction.

Mechanism of Manganese Ions Extraction Using ELM Technique

The mechanism of Mn ions extraction using the ELM technique is schematized in Fig. 6b. Mn^{2+} ion in the external phase reacts with the $(HL)_{x(org)}$ carrier, a protonated ion-exchange liquid extractor dissolved in the membrane phase, to form the $ML_n(HL)_{(mx-n)(org)}$ complex with the release of

H^+ (aq) or proton that enters the external phase. Then, the manganese complex passes through the membrane to the interface between the membrane phase and the internal phase containing concentrated H_2SO_4, where the stripping reaction occurs. The concentrated acid in the internal phase promotes the manganese ions release from the membrane phase into the internal phase. Instead, the internal acidic solution donates its protons to the carrier in the membrane phase, decreasing the concentration of the ML_n (HL) $_{(mx-n)(org)}$ at the interface of the internal phase. This sharp difference in the concentration of the manganese complex between the internal and external phases creates a strong driving force for transferring the manganese complex into the internal phase, which increases the extraction rate. In this method, the concentration of manganese ion in the internal phase can be 70 times higher than the external phase. Besides, the Fourier Transform Infrared spectroscopy (FTIR) analysis was performed to confirm the occurred Mn ions extraction, identifying the characteristic functional groups before and after the extraction process in the range of 500–4000 cm^{-1}.

As demonstrated in Fig. 6c, the IR spectra differed before and after Mn extraction due to the complexes' formation after extraction. In both spectra, the peaks at ~3380 cm^{-1} and ~3282 cm^{-1} can be ascribed to O–H stretching, suggesting Span80 and kerosene presence in the membrane [59]. In addition, a peak at 1740 cm^{-1} confirmed the presence of C=O stretching vibration associated with Span 80. Tween 80 presence was found in the membrane phase with the detection of N–H bending and C–N stretching peaks at 1468 cm^{-1}. The peak centered at 3640 cm^{-1} was assigned to O–H stretching [60]. The newly observed peak of the IR spectra after extraction at 2285.02 cm^{-1} could indicate the complex formation of manganese and Cyanex 272.

Manganese (II) Ion Extraction Using Design of Experiment

In this research, the CCD was used to optimize the number of experiments. In the Minitab 18 software, due to the use of a 1/2 level FFD screening step, the optimization was done with five different significant factors on the system and using a CCD of type 1/2. Eventually, a total number of 64 experiments (52 of them related to non-central points and 12 to central points) was suggested. The five major factors that were selected from the FFD design method included: carrier concentration, feed phase pH, feed phase/emulsion volume ratio, and W/O/W emulsion stirring rate and stirring time. For achieving acceptable accuracy, the experiments were repeated three times, at least. Table 1 shows the high and low levels of factors involved in the CCD experiment. Moreover, Table S4 presents the

Fig. 6 **a** Plot of log D versus log [Cyanex 272] (pH 4, O:A = 1:1); **b** A schematic representation of manganese ions extraction using ELM technique; **c** Comparison of FTIR spectra before and after the extraction process
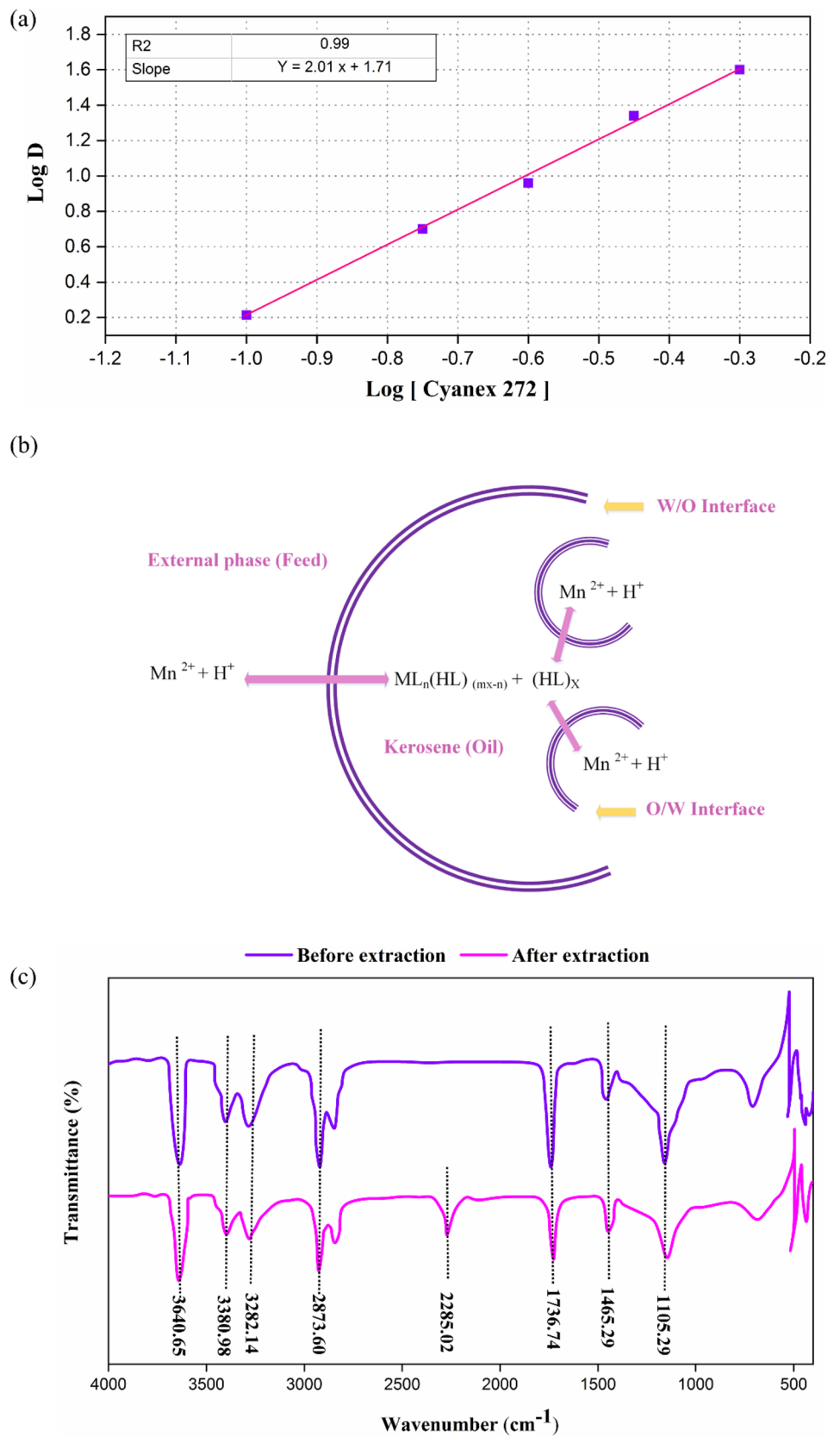
response matrix design results for the manganese recovery using the CCD method.

The residual plots (Fig. 7a–d) and ANOVA table (Table. S6) were used to evaluate the adequacy and accuracy of the models developed in the CCD, respectively. The residual plots should have the following characteristics: the normal probability plot should be linear, the residuals must be roughly independent of each other, their variance must be constant for all the different variable values, and there should not be a pattern in the plot of residuals vs the predicted values. The linear trend in Fig. 7a confirms that the data have a suitable distribution. There is no evident trend in Fig. 7b and d, which also confirms the model adequacy. Finally, in Fig. 7c (histogram), the residual changes should follow a normal distribution to indicate the data's adequacy [61].

ANOVA table was used to check the accuracy of the model. As reported in Table S6, the model's p value and the model's lack of fit were significant and insignificant, respectively, indicating the model accuracy and adequacy. In addition, the F value of the model (~ 37.7) confirms the meaningfulness of the model (less than 0.01% error). R^2 (adj) value in the sample is 87.49%, showing that the developed model covers $\sim 88\%$ of the data. With a thorough investigation of the diagrams and ANOVA table, it was concluded that the proposed model was suitable for investigating the factors affecting the response rate.

Equation 7 is used to predict the response based on the specified factors (e.g., factors X_1 to X_5 in Table S4) [62]:

$$Y = \beta_0 + \sum \beta_i X_i + \sum \beta_{ii} X_i^2 + \sum \beta_{ij} X_i X_j, \qquad (7)$$

where Y, β_0, β_i, β_{ii}, and β_{ij} are the predicted response (Mn extraction %), constant, linear coefficient, coefficient of the squared effects, and coefficient of the interaction effect, respectively. Equation 7 is solved in Minitab 18 software to estimate the coefficients. The meaningfulness of each sentence in the regressed equation (Eq. 7) is determined by the variance analysis (ANOVA) for each response. For any X_i^2 and $X_i X_j$ in Eq. 7, the related P value was estimated. In the cases with values greater than 0.05, the β_{ii} and β_{ij} coefficients were set to zero. The final form of Eq. 7 after analysis and regression is

$$\text{Manganese Removal} = 80.12 - 3.39_{X1} + 10.51_{X2} + 4.52_{X3} + 1.94_{X4} + 12.24_{X5}$$
$$- 2.98_{X1}^2 - 2665_{X2}^2 - 4.14_{X5}^2 - 2.66_{X1*X2}$$
$$- 2.99_{X2*X5} + 4.53_{X3*X4} - 3.17_{X3*X5} \qquad (8)$$
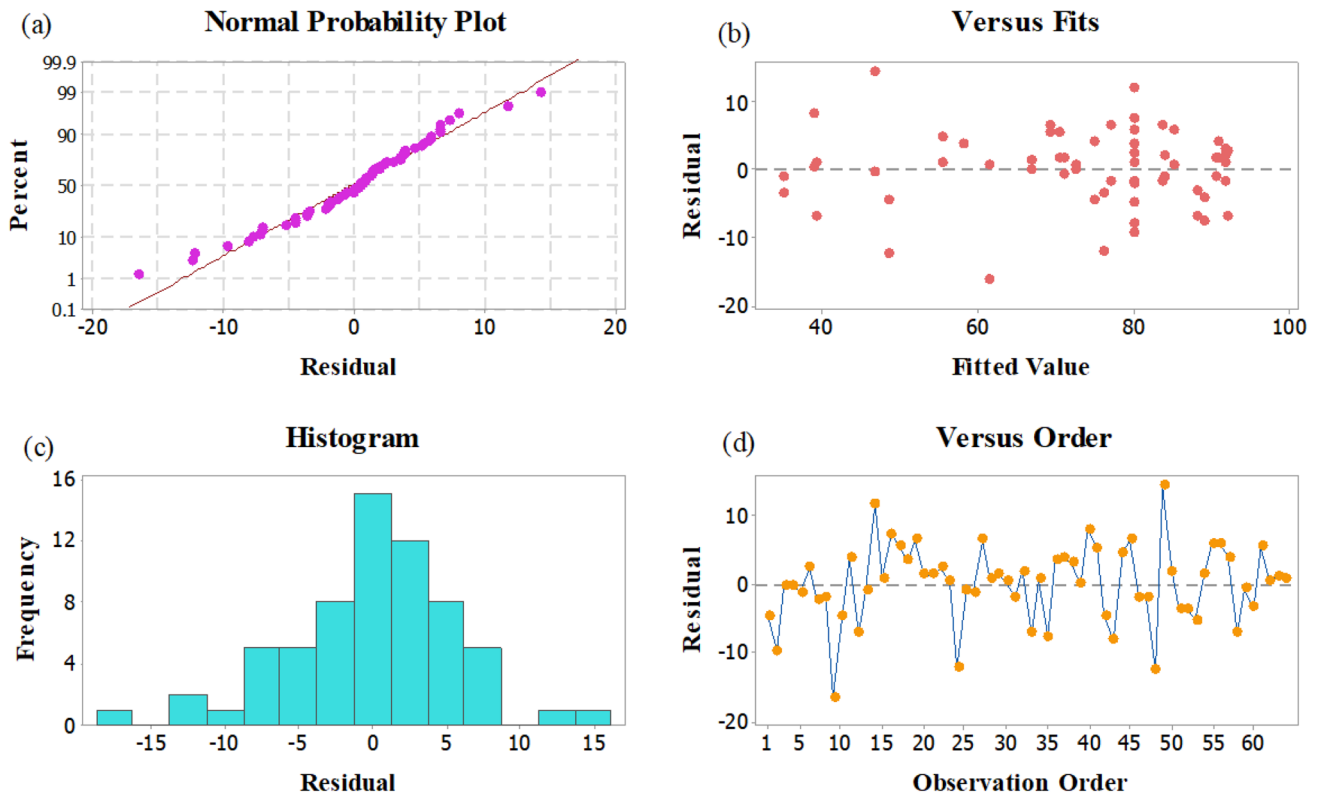
Fig. 7 Residual plot diagrams: **a** normal probability plot, **b** versus fits, **c** histogram, and **d** versus order for model adequacy in the CCD method

Table 2 Comparison among the values of the factor obtained under the optimum and three random conditions

Factors	Optimum condition	Random condition 1	Random condition 2	Random condition 3
X_1	3.23	4.624	3.036	3.010
X_2	6.90	7.688	7.968	7.847
X_3	3.96	4.894	4.158	4.611
X_4	16.70	19.465	17.139	13.517
X_5	442	533.147	456.137	539.345
Fitted result (% manganese removal)	100	98	100	100
Avg. test manganese removal	97.63	89.45	95.80	91.03
Error	2.37	8.55	4.2	8.97

Contour plots are shown in Fig. S2a–k. It should be noted that the highest removal in Fig. S2a was achieved when the carrier concentration (X_2) and emulsion/feed phase ratio (X_1) were approximately within 7–10 and 1–5, respectively. In contrast, in Fig. S2h, the least response was found for a W/O/W emulsion stirring rate (X_5) of less than 300 rpm with a carrier concentration (X_2) below 3 (wt%).

Three random conditions were chosen to check the accuracy of the software's proposed optimum conditions, and the optimum conditions were experimentally tested (Table 2). The results were then reported in Table 2 and Fig. S3, demonstrating that the highest removal was achieved via the optimum conditions suggested by the software.

Conclusions

In this work, a complete experimental protocol to demonstrate the feasibility of manganese ions removal from water via the ELM method was set up in three steps. In the first step, the physicochemical factors affecting the stability of the liquid membrane were investigated. Then, the FFD method was applied to identify the main parameters that can influence the manganese extraction, such as carrier concentration, emulsion-to-feed phase volume ratio, feed phase pH, water-in-oil-in-water (W/O/W) emulsion stirring time, and speed.

In the last step, after the determination of the appropriate factors range, the central composite design was used to optimize them, comparing the experimental results obtained via OFAT and DOE. The optimized results showed that with the emulsion volume/feed phase ratio ~ 3, carrier concentration ~ 8, feed phase pH ~ 4, W/O/W emulsion stirring duration ~ 17 min, and W/O/W emulsion stirring rate ~ 450, and the highest extraction rate (~ 97%) can be achieved.

In conclusion, the proposed and developed experimental protocol could be considered as an easy and efficient tool for identifying the optimal parameter in the Mn water extraction by ELM, paving the way for applications to other heavy metals, with significant impacts from the environmental point of view.

Author Contributions IS: Conceptualization, investigation, experimental work, gathering data, and preparing the original draft. AS: Supervision, development of the research methodology, data analyzing, and preparing the paper. AB: methodology development, writing, reviewing, and editing the manuscript. IC: Supervision, reviewing and editing the manuscript, and preparation of the final version.

Declarations

Conflict of interest All authors state that there is no conflict of interest.

References

1. Wuana RA, Okieimen FE (2011) Heavy metals in contaminated soils: a review of sources, chemistry, risks and best available strategies for remediation. ISRN Ecol 2011:20. https://doi.org/10.5402/2011/402647
2. Ma H, Kökkılıç O, Waters KE (2017) The use of the emulsion liquid membrane technique to remove copper ions from aqueous systems using statistical experimental design. Miner Eng 107:88–99
3. Tan Z, Mei G, Li W, Zeng K, Liang R, Zeng X (2004) Metallurgy of manganese. Central South University Press, Changsha
4. Swain B, Jeong J, Kim S-k, Lee J-c (2010) Separation of platinum and palladium from chloride solution by solvent extraction using Alamine 300. Hydrometallurgy 104(1):1–7. https://doi.org/10.1016/j.hydromet.2010.03.013
5. Li Y, Shahbazi A, Williams K, Wan C (2008) Separate and concentrate lactic acid using combination of nanofiltration and reverse osmosis membranes. Appl Biochem Biotechnol 147(1):1–9. https://doi.org/10.1007/s12010-007-8047-5

6. Wojtyniak B, Kołodziejczyk J, Szaniawska D (2016) Production of lactic acid by ultrafiltration of fermented whey obtained in bioreactor equipped with ZOSS membrane. Chem Eng J 305:28–36. https://doi.org/10.1016/j.cej.2016.01.048

7. Joglekar HG, Rahman I, Babu S, Kulkarni BD, Joshi A (2006) Comparative assessment of downstream processing options for lactic acid. Sep Purif Technol 52(1):1–17. https://doi.org/10.1016/j.seppur.2006.03.015

8. Feng M, Wenzel M, Wang S, Du H, Zhang Y, Weigand JJ (2021) Separation of Na3VO4 and Na2CrO4 from high alkalinity solutions by solvent extraction. Sep Purif Technol 255:117282. https://doi.org/10.1016/j.seppur.2020.117282

9. Chen K, Hao S, Lyu H, Luo G, Zhang S, Chen J (2017) Ion exchange separation for recovery of monosaccharides, organic acids and phenolic compounds from hydrolysates of lignocellulosic biomass. Sep Purif Technol 172:100–106. https://doi.org/10.1016/j.seppur.2016.08.004

10. Kumar A, Thakur A, Panesar PS (2019) A review on emulsion liquid membrane (ELM) for the treatment of various industrial effluent streams. Rev Environ Sci Bio/Technol 18(1):153–182. https://doi.org/10.1007/s11157-019-09492-2

11. Salahshoori I, Nasirian D, Rashidi N, Hossain MK, Hatami A, Hassanzadeganroudsari M (2020) The effect of silica nanoparticles on polysulfone–polyethylene glycol (PSF/PEG) composite membrane on gas separation and rheological properties of nanocomposites. Polym Bull. https://doi.org/10.1007/s00289-020-03255-8

12. Hatami A, Salahshoori I, Rashidi N, Nasirian D (2020) The effect of ZIF-90 particle in Pebax/Psf composite membrane on the transport properties of CO2, CH4 and N2 gases by Molecular Dynamics Simulation method. Chin J Chem Eng 28(9):2267–2284. https://doi.org/10.1016/j.cjche.2019.12.011

13. Nasirian D, Salahshoori I, Sadeghi M, Rashidi N, Hassanzadeganroudsari M (2020) Investigation of the gas permeability properties from polysulfone/polyethylene glycol composite membrane. Polym Bull 77(10):5529–5552. https://doi.org/10.1007/s00289-019-03031-3

14. Salahshoori I, Babapoor A, Seyfaee A (2021) Elevated performance of the neat, hybrid and composite membranes by the addition of nanoparticles (ZIF-67): a molecular dynamics study. Polym Bull. https://doi.org/10.1007/s00289-021-03673-2

15. Salahshoori I, Seyfaee A, Babapoor A, Neville F, Moreno-Atanasio R (2021) Evaluation of the effect of silica nanoparticles, temperature and pressure on the performance of PSF/PEG/SiO2 mixed matrix membranes: a molecular dynamics simulation (MD) and design of experiments (DOE) study. J Mol Liq 333:115957. https://doi.org/10.1016/j.molliq.2021.115957

16. San Román MF, Bringas E, Ibañez R, Ortiz I (2010) Liquid membrane technology: fundamentals and review of its applications. J Chem Technol Biotechnol 85(1):2–10. https://doi.org/10.1002/jctb.2252

17. Pfeiffer RM, Bunge AL (2020) Leakage and swell in emulsion liquid membrane systems: comparing continuous stirred-tank reactor and batch experiments. J Ind Eng Chem 87:68–77. https://doi.org/10.1016/j.jiec.2020.03.013

18. Ahmad AL, Kusumastuti A, Derek CJC, Ooi BS (2011) Emulsion liquid membrane for heavy metal removal: an overview on emulsion stabilization and destabilization. Chem Eng J 171(3):870–882. https://doi.org/10.1016/j.cej.2011.05.102

19. Björkegren S, Karimi FR, Martinelli A, Jayakumar SN, Hashim AM (2015) A new emulsion liquid membrane based on a palm oil for the extraction of heavy metals. Membranes. https://doi.org/10.3390/membranes5020168

20. Mondal S, Purkait MK, De S (2018) Emulsion Liquid Membrane. In: Mondal S, Purkait MK, De S (eds) Advances in dye removal technologies. Springer Singapore, Singapore, pp 313–323

21. Raghuraman B, Tirmizi N, Wiencek J (1994) Emulsion liquid membranes for wastewater treatment: equilibrium models for some typical metal-extractant systems. Environ Sci Technol 28(6):1090–1098. https://doi.org/10.1021/es00055a018

22. Kumar A, Thakur A, Panesar PS (2018) Lactic acid extraction using environmentally benign Green emulsion ionic liquid membrane. J Clean Prod 181:574–583. https://doi.org/10.1016/j.jclepro.2018.01.263

23. Reis MTA, de Freitas OMF, Ismael MRC, Carvalho JMR (2007) Recovery of phenol from aqueous solutions using liquid membranes with Cyanex 923. J Membr Sci 305(1):313–324. https://doi.org/10.1016/j.memsci.2007.08.016

24. Abbassian K, Kargari A (2016) Modification of membrane formulation for stabilization of emulsion liquid membrane for extraction of phenol from aqueous solutions. J Environ Chem Eng 4(4):3926–3933. https://doi.org/10.1016/j.jece.2016.08.030

25. Salahshoori I, Hatami A, Seyfaee A (2020) Investigation of experimental results and D-optimal design of hafnium ion extraction from aqueous system using emulsion liquid membrane technique. J Iran Chem Soc. https://doi.org/10.1007/s13738-020-02007-9

26. Valenzuela F, Cabrera J, Basualto C, Sapag J, Romero J, Sánchez J, Rios G (2007) Separation of zinc ions from an acidic mine drainage using a stirred transfer cell-type emulsion liquid membrane contactor. Sep Sci Technol 42(2):363–377. https://doi.org/10.1080/01496390601069887

27. Shirasangi R, Kohli HP, Gupta S, Chakraborty M (2020) Separation of Methylparaben by emulsion liquid membrane: optimization, characterization, stability and multiple cycles studies. Colloids Surf A 597:124761

28. Davoodi-Nasab P, Rahbar-Kelishami A, Safdari J, Abolghasemi H (2017) Application of emulsion nanofluids membrane for the extraction of gadolinium using response surface methodology. J Mol Liq 244:368–373

29. Raji M, Abolghasemi H, Safdari J, Kargari A (2018) Response surface optimization of dysprosium extraction using an emulsion liquid membrane integrated with multi-walled carbon nanotubes. Chem Eng Technol 41(9):1857–1870

30. Wagner JR, Mount EM, Giles HF (2014) 25 - Design of experiments. In: Wagner JR, Mount EM, Giles HF (eds) Extrusion, 2nd edn. William Andrew Publishing, Oxford, pp 291–308

31. Carley KM, Kamneva NY, Reminga J (2004) Response surface methodology. Carnegie-Mellon Univ Pittsburgh PA School of Computer Science, CASOS Technical Report, CMU-ISRI-04-136

32. Sahu NK, Andhare A (2018) Design of experiments applied to industrial process. Stat Approach Emphasis Des Exp Appl Chem Process 5:353–368

33. Kargari A, Kaghazchi T, Sohrabi M, Soleimani M (2004) Batch extraction of gold(III) ions from aqueous solutions using emulsion liquid membrane via facilitated carrier transport. J Membr Sci 233(1):1–10. https://doi.org/10.1016/j.memsci.2003.09.027

34. Li N, Cahn R, Naden D, Lai R (1983) Liquid membrane processes for copper extraction. Hydrometallurgy 9(3):277–305

35. Patnaik P (1995) Liquid emulsion membranes: principles, problems and applications in fermentation processes. Biotechnol Adv 13(2):175–208

36. Laki S, Arabi Shamsabadi A, Madaeni SS, Niroomanesh M (2015) Separation of manganese from aqueous solution using an emulsion liquid membrane. RSC Adv 5(102):84195–84206. https://doi.org/10.1039/C5RA08547K

37. Othman N, Mat H, Goto M (2006) Separation of silver from photographic wastes by emulsion liquid membrane system. J Membr Sci 282(1):171–177. https://doi.org/10.1016/j.memsci.2006.05.020

38. Sabry R, Hafez A, Khedr M, El-Hassanin A (2007) Removal of lead by an emulsion liquid membrane: Part I. Desalination 212(1–3):165–175

39. Kageyama T, Matsumiya H, Hiraide M (2004) Separation of traces of heavy metals from an iron matrix by use of an emulsion liquid membrane. Anal Bioanal Chem 379:1083–1087. https://doi.org/10.1007/s00216-004-2669-z

40. Fouad EA (2008) Zinc and copper separation through an emulsion liquid membrane containing Di-(2-Ethylhexyl) phosphoric acid as a carrier. Chem Eng Technol 31(3):370–376

41. Gasser MS, El-Hefny NE, Daoud JA (2008) Extraction of Co(II) from aqueous solution using emulsion liquid membrane. J Hazard Mater 151(2):610–615. https://doi.org/10.1016/j.jhazmat.2007.06.032

42. Wan Y, Zhang X (2002) Swelling determination of W/O/W emulsion liquid membranes. J Membr Sci 196(2):185–201

43. Chakraborty M, Bhattacharya C, Datta S (2010) Emulsion liquid membranes: Definitions and classification, theories, module design, applications, new directions and perspectives. In: Kislik VS (ed) Liquid membranes. Elsevier, Amsterdam, pp 141–199

44. Basualto C, Poblete M, Marchese J, Ochoa A, Acosta A, Sapag J, Valenzuela F (2006) Extraction of cadmium from aqueous solutions by emulsion liquid membranes using a stirred transfer cell contactor. J Braz Chem Soc 17(7):1347–1354

45. Rosly MB, Jusoh N, Othman N, Rahman HA, Sulaiman RNR, Noah NFM (2020) Stability of emulsion liquid membrane using bifunctional diluent and blended nonionic surfactant for phenol removal. Chem Eng Process 148:107790. https://doi.org/10.1016/j.cep.2019.107790

46. Lv G, Wang F, Cai W, Zhang X (2014) Characterization of the addition of lipophilic Span 80 to the hydrophilic Tween 80-stabilized emulsions. Colloids Surf A 447:8–13. https://doi.org/10.1016/j.colsurfa.2014.01.066

47. Gasser M, El-Hefny N, Daoud J (2008) Extraction of Co (II) from aqueous solution using emulsion liquid membrane. J Hazard Mater 151(2–3):610–615

48. Seyfaee A, Neville F, Moreno-Atanasio R (2015) Experimental results and theoretical modeling of the growth kinetics of polyamine-derived silica particles. Ind Eng Chem Res 54(9):2466–2475

49. Liu H, Zhang Y-m, Huang J, Liu T, Xue N-n, Shi Q-h (2017) Optimization of vanadium (IV) extraction from stone coal leaching solution by emulsion liquid membrane using response surface methodology. Chem Eng Res Des 123:111–119. https://doi.org/10.1016/j.cherd.2017.05.001

50. Chakraborty M, Bhattacharya C, Datta S (2003) Mass transfer analysis of the extraction of nickel (II) by emulsion liquid membrane. Indian J Chem Technol 10:311–320

51. Peng W, Jiao H, Shi H, Xu C (2012) The application of emulsion liquid membrane process and heat-induced demulsification for removal of pyridine from aqueous solutions. Desalination 286:372–378. https://doi.org/10.1016/j.desal.2011.11.051

52. Peralta-Martínez MV, Arriola-Medellín A, Manzanares-Papayanopoulos E, Sánchez-Sánchez R, Palacios-Lozano EM (2004) Influence of the speed mixing-on viscosity and droplet size of oil in water emulsions. Pet Sci Technol 22(7–8):1035–1043

53. Nurdin S, Suli LNM, Nour AH, Rizauddin D, Gimbun J, Nurdin S (2014) Stabilization and characterization of heavy crude oil in water (o/w) emulsions. IJRET 3(2):489–496

54. Muschiolik G, Dickinson E (2017) Double emulsions relevant to food systems: preparation, stability, and applications. Compr Rev Food Sci Food Saf 16(3):532–555

55. Chakrabarty K, Saha P, Ghoshal AK (2010) Separation of lignosulfonate from its aqueous solution using emulsion liquid membrane. J Membr Sci 360(1):34–39. https://doi.org/10.1016/j.memsci.2010.04.043

56. Mohammed AA, Selman HM (2019) Extraction of lead ions from aqueous solution by CO-stabilization mechanisms of magnetic Fe2O3 particles and nonionic surfactants in emulsion liquid membrane. Colloids Surf A. https://doi.org/10.1016/j.colsurfa.2019.02.018

57. Mohammed AA, Selman HM, Abukhanafer G (2018) Liquid surfactant membrane for lead separation from aqueous solution: studies on emulsion stability and extraction efficiency. J Environ Chem Eng 6(6):6923–6930. https://doi.org/10.1016/j.jece.2018.10.021

58. Kankekar PS, Wagh SJ, Mahajani VV (2010) Process intensification in extraction by liquid emulsion membrane (LEM) process: a case study; enrichment of ruthenium from lean aqueous solution. Chem Eng Process 49(4):441–448. https://doi.org/10.1016/j.cep.2010.02.005

59. Roy Choudhury S, Mandal Bera A, Chkaravorty D, Gopal M, Goswami A (2013) Evaluation of physicochemical properties, and antimicrobial efficacy of monoclinic sulfur-nanocolloid. J Nanopart Res 15:1–11. https://doi.org/10.1007/s11051-013-1491-y

60. Ludvigsson M, Lindgren J, Tegenfeldt J (2000) FTIR study of water in cast Nafion films. Electrochim Acta 45(14):2267–2271. https://doi.org/10.1016/S0013-4686(99)00438-7

61. Ahn H (2015) Central composite design for the experiments with replicate runs at factorial and axial points. In: Industrial engineering, management science and applications, Berlin, Heidelberg, pp. 969–979. https://doi.org/10.1007/978-3-662-47200-2_101.

62. Bezerra MA, Santelli RE, Oliveira EP, Villar LS, Escaleira LA (2008) Response surface methodology (RSM) as a tool for optimization in analytical chemistry. Talanta 76(5):965–977. https://doi.org/10.1016/j.talanta.2008.05.019

Authors and Affiliations

Iman Salahshoori[1] · Ahmad Seyfaee[2] · Aziz Babapoor[3] · Ilaria Cacciotti[4]

✉ Ahmad Seyfaee
ahmad.seyfaee@adelaide.edu.au

✉ Ilaria Cacciotti
ilaria.cacciotti@unicusano.it

1 Department of Chemical Engineering, Science and Research Branch, Islamic Azad University, Tehran, Iran

2 School of Mechanical Engineering, University of Adelaide, Adelaide, Australia

3 Department of Chemical Engineering, University of Mohaghegh Ardabili, Ardabil, Iran

4 Department of Engineering, INSTM RU, University of Rome "Niccolò Cusano", via Don Carlo Gnocchi 3, 00166 Rome, Italy